Contents

VIP ***The following Communications have been judged by at least two referees to be "very important papers" and will be published online at www.angewandte.org soon:***

T. A. Rokob, A. Hamza, A. Stirling, T. Soós, I. Pápai**
Turning Frustration into Bond Activation: A Theoretical Mechanistic Study on Heterolytic Hydrogen Splitting by Frustrated Lewis Pairs

*E. Stavitski, M. H. Kox, I. Swart, F. M. de Groot, B. M. Weckhuysen**
In Situ Synchrotron-Based IR Microspectroscopy To Study Catalytic Reactions in Zeolite Crystals

*C. Ruspic, J. R. Moss, M. Schürmann, S. Harder**
Remarkable Stability of Metallocenes with Superbulky Ligands: Spontaneous Reduction of Sm^{III} to Sm^{II}

*L. M. Fidalgo, G. Whyte, D. Bratton, C. F. Kaminski, C. Abell, W. T. S. Huck**
From Microdroplets to Microfluidics: Selective Emulsion Separation in Microfluidic Devices

I. Paterson, E. A. Anderson, S. M. Dalby, J. Ho Lim, J. Genovino, P. Maltas, C. Moessner*
Total Synthesis of Spirastrellolide A Methyl Ester—Part 1: Synthesis of an Advanced C17–C40 Bis(spiroacetal) Subunit

I. Paterson, E. A. Anderson, S. M. Dalby, J. Ho Lim, J. Genovino, P. Maltas, C. Moessner*
Total Synthesis of Spirastrellolide A Methyl Ester—Part 2: Subunit Union and Completion of the Synthesis

Books

Essentials of Carbohydrate Chemistry and Biochemistry — Thisbe K. Lindhorst — *reviewed by A. Hoffmann-Röder* ____ 1360

Quality Assurance for the Analytical Chemistry Laboratory — D. Brynn Hibbert — *reviewed by M. Vogel* ____ 1360

Highlights

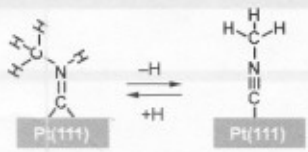

Realization of a dream: The scanning tunneling microscope is not only capable of imaging and manipulating adsorbed species, it can be used for vibrational spectroscopy on these species. With this method, a full reaction cycle was investigated in which methylaminocarbyne on Pt(111) was dehydrogenated and rehydrogenated (see scheme). This method is expected to be instrumental in the understanding of fundamental phenomena in heterogeneous catalysis.

Surface Chemistry

C. Wöll* ____ 1364 – 1366

Spectroscopic Characterization and Deliberate Modification of a Single Molecule by Tunneling of Electrons

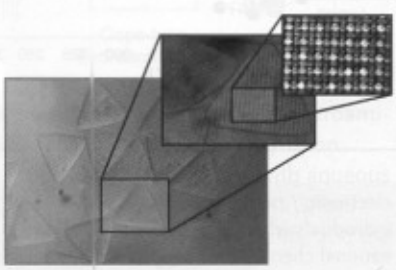

Assembly-line microparticles: An innovative approach for the high-throughput fabrication of complex three-dimensional and chemically anisotropic microstructures is highlighted (illustrated: patterned triangles with edges of circa 60 μm) based on the synergistic use of stop-flow interference lithography and microfluidics.

Microfabrication

R. S. Kane* ____ 1368 – 1370

Fabricating Complex Polymeric Micro- and Nanostructures: Lithography in Microfluidic Devices

© 2008 Wiley-VCH Verlag GmbH & Co. KGaA, Weinheim

Contents

Minireviews

Supramolecular Assemblies

J. Moussa, H. Amouri* ____ 1372 – 1380

Supramolecular Assemblies Based on Organometallic Quinonoid Linkers: A New Class of Coordination Networks

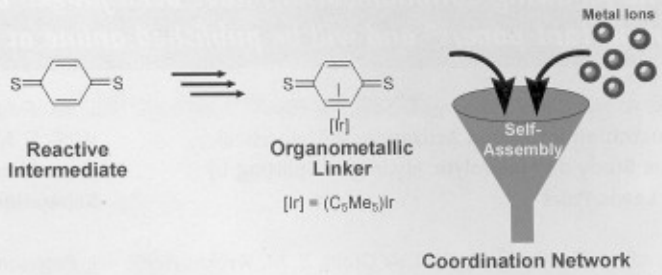

A new family of coordination networks self-assembles from individual components using metalated quinonoid and thioquinonoid linkers (see scheme). These novel assemblies exhibit short π–π and M···M interactions. The wide range of new architectures illustrates the role of the organometallic linkers in promising compounds for the development of functional materials.

Reviews

Nucleic Acid Carriers

V. Sokolova, M. Epple* ____ 1382 – 1395

Inorganic Nanoparticles as Carriers of Nucleic Acids into Cells

Particularly useful: Many different kinds of nanoparticles are readily taken up by living cells (see picture; nanoparticles can be seen as red dots inside the cell) and thereby can be used as carriers for nucleic acids (DNA, siRNA) to change the genetic arsenal of a cell. Clinically, this is of interest to treat genetically caused diseases (so called "gene therapy").

Communications

Negative Thermal Expansion

A. E. Phillips, A. L. Goodwin, G. J. Halder, P. D. Southon, C. J. Kepert* 1396 – 1399

Nanoporosity and Exceptional Negative Thermal Expansion in Single-Network Cadmium Cyanide

Accentuate the negative: Single-network cadmium cyanide displays isotropic negative thermal expansion behavior of unprecedented magnitude over a large temperature range (see graph of unit cell parameter *a* versus temperature). Guest molecules in the pores of this framework block the transverse vibrational modes responsible for this behavior, causing the value of the linear coefficient of thermal expansion to increase with guest occupancy.

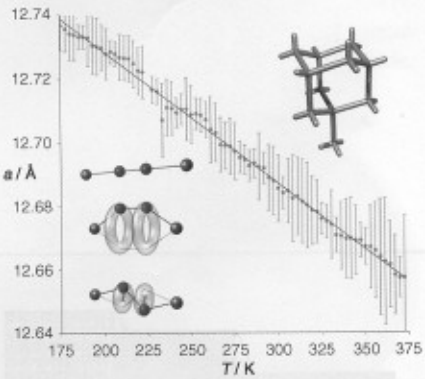

For the USA and Canada:
ANGEWANDTE CHEMIE International Edition (ISSN 1433-7851) is published weekly by Wiley-VCH, PO Box 191161, 69451 Weinheim, Germany. Air freight and mailing in the USA by Publications Expediting Inc., 200 Meacham Ave., Elmont, NY 11003. Periodicals postage paid at Jamaica, NY 11431. US POSTMASTER: send address changes to *Angewandte Chemie*, Wiley-VCH, 111 River Street, Hoboken, NJ 07030. Annual subscription price for institutions: US$ 7225/6568 (valid for print and electronic / print or electronic delivery); for individuals who are personal members of a national chemical society prices are available on request. Postage and handling charges included. All prices are subject to local VAT/sales tax.

© 2008 Wiley-VCH Verlag GmbH & Co. KGaA, Weinheim

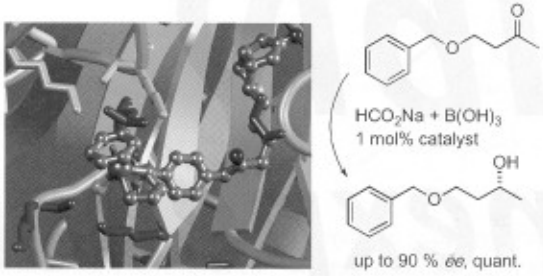

A structure is worth a thousand words: Guided by the X-ray structure of an *S*-selective artificial transfer hydrogenase, designed evolution was used to optimize the selectivity of hybrid catalysts. Fine-tuning of the second coordination sphere of the ruthenium center (see picture, orange sphere) by introduction of two point mutations allowed the identification of selective artificial transfer hydrogenases for the reduction of dialkyl ketones.

Artificial Metalloenzymes

M. Creus, A. Pordea, T. Rossel, A. Sardo, C. Letondor, A. Ivanova, I. LeTrong, R. E. Stenkamp,* T. R. Ward* ——— **1400 – 1404**

X-Ray Structure and Designed Evolution of an Artificial Transfer Hydrogenase

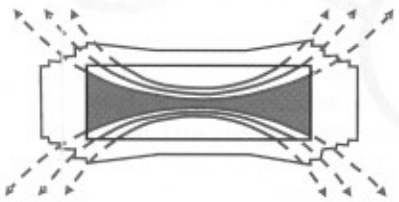

Taking shape: The 3D arrangement of a biomimetic fluorapatite–gelatine composite consists of elementary dipoles on the nanometer scale. The dipole field developed during growth of the composite causes formation and inclusion of gelatine microfibrils, which line up in the direction of the developing electric field. This microfibril pattern is the intrinsic code for development from an elongated hexagonal prism into a dumbbell morphology (see picture).

Biomineralization

R. Kniep,* P. Simon ——— **1405 – 1409**

"Hidden" Hierarchy of Microfibrils within 3D-Periodic Fluorapatite–Gelatine Nanocomposites: Development of Complexity and Form in a Biomimetic System

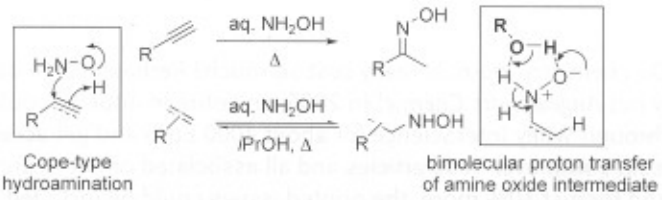

Keep it simple! Intermolecular hydroamination can be achieved simply upon heating alkynes and alkenes with aqueous hydroxylamine. Alkynes react to afford oximes in good to excellent yields, and the formation of Markovnikov products is favored. A mechanism involving Cope-type hydroamination followed by bimolecular proton transfer is suggested and supported by DFT studies.

Hydroamination

A. M. Beauchemin,* J. Moran, M.-E. Lebrun, C. Séguin, E. Dimitrijevic, L. Zhang, S. I. Gorelsky ——— **1410 – 1413**

Intermolecular Cope-Type Hydroamination of Alkenes and Alkynes

© 2008 Wiley-VCH Verlag GmbH & Co. KGaA, Weinheim

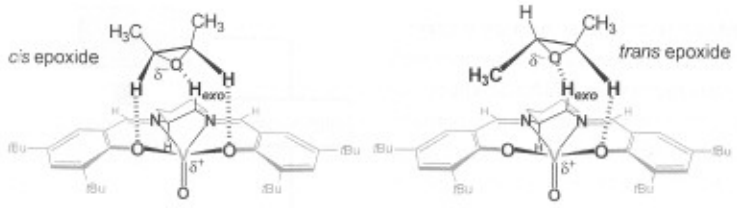

EPR and ENDOR spectroscopies combined with DFT calculations have revealed the selective binding of a *cis* over a *trans* epoxide to a chiral vanadyl salen complex (see picture). Complementary DFT calculations identified a weak electrostatic interaction supplemented by multiple hydrogen-bonding contacts as the origins of this selectivity. These observations were experimentally confirmed in frozen solution by orientation selective ENDOR measurements.

ENDOR spectroscopy

D. M. Murphy,* I. A. Fallis,* D. J. Willock,* J. Landon, E. Carter, E. Vinck **1414 – 1416**

Discrimination of Geometrical Epoxide Isomers by ENDOR Spectroscopy and DFT Calculations: The Role of Hydrogen Bonds

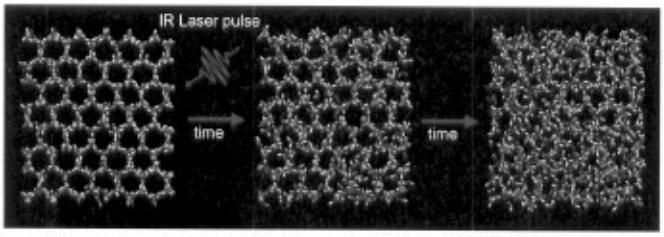

Cold as ice: Molecular dynamics simulation provides snapshots of a melting ice crystal (see picture). The laser pulse heats up the system, and the energy is absorbed in the O–H bonds. After a few picoseconds, the energy is transferred to rotational and translational energy, causing the crystal to melt. The melting starts as a nucleation process, and even long after the first melting is initialized, pockets of crystalline structures can be found.

Molecular Dynamics Simulations

C. Caleman, D. van der Spoel* **1417 – 1420**

Picosecond Melting of Ice by an Infrared Laser Pulse: A Simulation Study

Nanopatterns: The feasibility of a new lithographic technique, chemical lithography with self-assembled monolayers (SAMs) of commercially available aliphatic compounds as resist materials, is demonstrated by the fabrication of polymer nanopatterns (see image). The technique is based on an irradiation-promoted exchange reaction. Patterning requires a much lower dose than electron-beam chemical lithography with aromatic SAMs as resists.

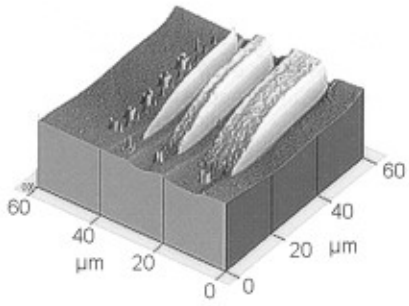

Chemical Lithography

N. Ballav, S. Schilp, M. Zharnikov* **1421 – 1424**

Electron-Beam Chemical Lithography with Aliphatic Self-Assembled Monolayers

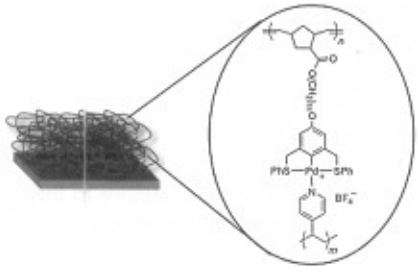

Metal–ligand interactions can be used to create coordination polymer multilayers (see picture). Growth is linear with layer and bilayer number, and the bilayer thickness depends on deposition concentration. This approach combines the stability of covalent multilayers with the responsiveness of polyelectrolyte-based multilayers.

Polymer Multilayers

C. R. South, V. Piñón III, M. Weck* **1425 – 1428**

Erasable Coordination Polymer Multilayers on Gold

© 2008 Wiley-VCH Verlag GmbH & Co. KGaA, Weinheim

Contents

Biotechnology

Y. Okubo, K. Ikemoto,* K. Koike, C. Tsutsui, I. Sakata, O. Takei, A. Adachi, T. Sakai* ——— **1429 – 1431**

DNA Introduction into Living Cells by Water Droplet Impact with an Electrospray Process

Charged water droplets from an electrospray device can generate a transient hole in cell membranes for DNA transport into a living cell. The number of cells containing DNA encoded with green fluorescent protein (GFP) increases with an increase in applied voltage. The technique can be applied to gene transfection to eukaryotic cells, tissues, and prokaryotic cells.

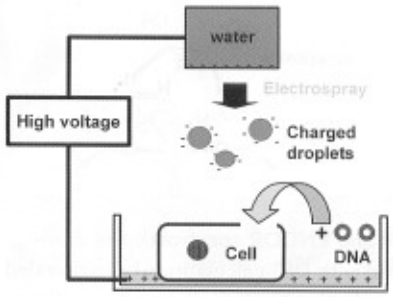

Natural Product Synthesis

K. C. Nicolaou,* J. Wang, Y. Tang ——— **1432 – 1435**

Synthesis of the Sporolide Ring Framework through a Cascade Sequence Involving an Intramolecular [4+2] Cycloaddition Reaction of an *o*-Quinone

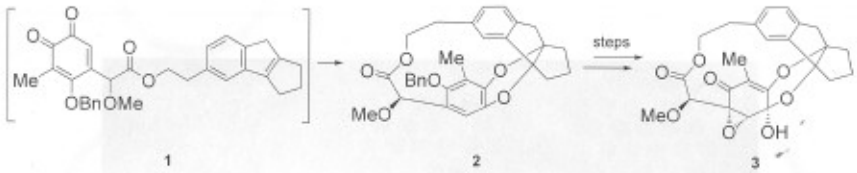

Sea-ing is believing: The *o*-quinone indene intermediate **1** was generated from the corresponding catechol substrate and converted into macrocycle **2** by a cascade sequence involving a novel intramolecular [4+2] cycloaddition reaction. This sequence serves as the key process to form the core heptacyclic structure **3** of the marine-derived natural products sporolide A and B, which were isolated from the relevant actinomycete fermentation broths.

Natural Product Synthesis

A. Biechy, S. Hachisu, B. Quiclet-Sire, L. Ricard, S. Z. Zard* ——— **1436 – 1438**

The Total Synthesis of (±)-Fortucine and a Revision of the Structure of Kirkine

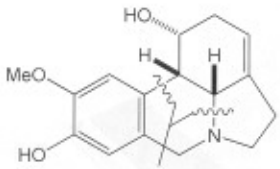

bonds formed in radical cascade fortucine

A molecular zipper: The total synthesis of the natural product fortucine relies on a radical cascade process initiated by the generation of a nitrogen-centered (amidyl) radical (see picture). The procedure is concise, and tin-free, as well as stereo- and regioselective. This synthesis has enabled the correction of the structure of kirkine, and the strategy represents a general and rapid entry into the galanthan framework.

Asymmetric Catalysis

Y. Wang, J. Wolf, P. Zavalij, M. P. Doyle* ——— **1439 – 1442**

Cationic Chiral Dirhodium Carboxamidates Are Activated for Lewis Acid Catalysis

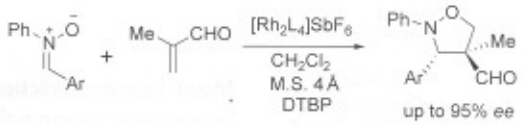

up to 95% *ee*

The power of a positive charge: Oxidized chiral dirhodium carboxamidate salts increase the rate of reaction of selected aldehydes with the Danishefsky diene (hetero-Diels–Alder reaction) and with nitrones (1,3-dipolar cycloaddition; see scheme, L = (*R*)-menthyl-2-oxopyrrolidine-(5*S*)-carboxylate, DTBP = 2,6-di-*tert*-butylpyridine). These cationic catalysts enhance enantiocontrol relative to their neutral dirhodium(II) counterparts.

© 2008 Wiley-VCH Verlag GmbH & Co. KGaA, Weinheim

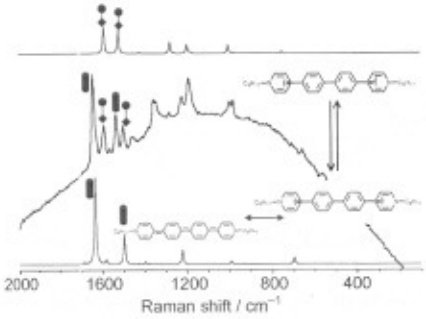

Raman marks of the singlet and triplet biradical species of an extended viologen are resolved in spite of the efficient intersystem crossing promoted by the quasi-isoenergetic locations of the lowest singlet and triplet states. Variable-temperature Raman measurements (see spectra) are instrumental for discriminating between the species, which rapidly interconvert their spin states.

Raman Detection of Biradicals

J. Casado,* S. Patchkovskii,*
M. Z. Zgierski, L. Hermosilla, C. Sieiro,
M. Moreno Oliva,
J. T. López Navarrete* ____ 1443 – 1446

Raman Detection of "Ambiguous" Conjugated Biradicals: Rapid Thermal Singlet-to-Triplet Intersystem Crossing in an Extended Viologen

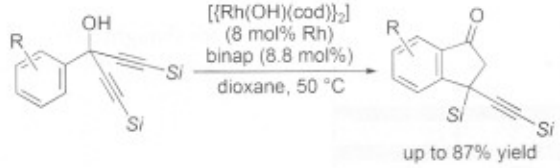

Ten little indanones: The title reaction (see scheme; *Si* = trialkylsilyl) is proposed to go through a pathway involving a β-carbon elimination/carborhodation sequence. Ready access to the carbinol substrates from an aromatic ester and a terminal alkyne makes the present catalysis reaction an efficient way of preparing 3-alkynyl-1-indanones.

Carborhodation

R. Shintani,* K. Takatsu, T. Katoh,
T. Nishimura, T. Hayashi* ___ 1447 – 1449

Rhodium-Catalyzed Rearrangement of Aryl Bis(alkynyl) Carbinols to 3-Alkynyl-1-indanones

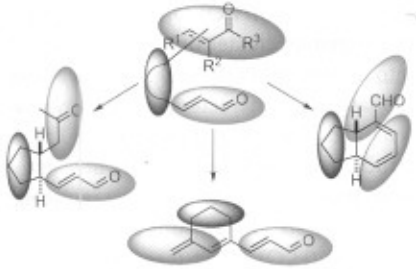

Various linked unsaturated dicarbonyl compounds were cyclized by dienamine catalysis. Depending on the substrates, alternative pathways were observed, leading to mono- and bicyclic products in high enantiomeric excess.

Asymmetric Synthesis

R. M. de Figueiredo, R. Fröhlich,
M. Christmann* _____ 1450 – 1453

Amine-Catalyzed Cyclizations of Tethered α,β-Unsaturated Carbonyl Compounds

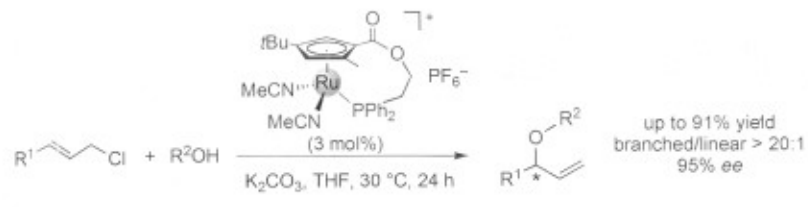

Design of an asymmetric catalyst: The planar-chiral cyclopentadienyl ruthenium complex shown in the scheme effectively catalyzes the reactions of unsymmetrically substituted allyl halides with phenol and alcohol to give the corresponding branched allyl ethers with high regio- and enantioselectivity.

Asymmetric Catalysis

K. Onitsuka,* H. Okuda,
H. Sasai _____ 1454 – 1457

Regio- and Enantioselective O-Allylation of Phenol and Alcohol Catalyzed by a Planar-Chiral Cyclopentadienyl Ruthenium Complex

© 2008 Wiley-VCH Verlag GmbH & Co. KGaA, Weinheim

Contents

Photochromic Complexes

N. V. Mockus, D. Rabinovich, J. L. Petersen, J. J. Rack* ____ **1458 – 1461**

Femtosecond Isomerization in a Photochromic Molecular Switch

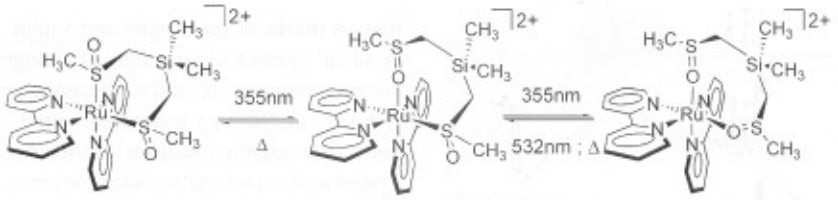

Back and forth: Irradiation in the metal-to-ligand charge transfer band of the bis S-bonded complex shown (see scheme, left) yields the mixed S,O isomer and then the O,O isomer in two subsequent excited-state reactions. Excitation of the S,O isomer at 355 nm yields the O,O isomer, while 532-nm excitation of the O,O isomer yields the S,O isomer. Isomerization occurs on a femto- to picosecond time-scale, demonstrating two-color photonic switching.

Methane Oxidation

A. Tomita, J. Nakajima, T. Hibino* ____ **1462 – 1464**

Direct Oxidation of Methane to Methanol at Low Temperature and Pressure in an Electrochemical Fuel Cell

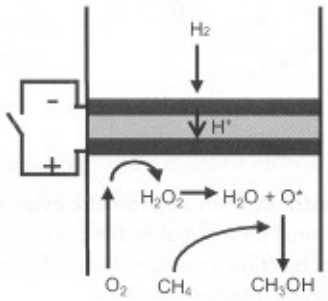

Fuel for thought? The direct oxidation of methane to methanol occurs at atmospheric pressure between 50 and 250 °C in a fuel-cell-type reactor (see picture). The efficiency of the electrochemical activation of oxygen is higher than that for the catalytic activation of oxygen.

Polythiooxometalates

M. N. Sokolov, I. V. Kalinina, E. V. Peresypkina, E. Cadot, S. V. Tkachev, V. P. Fedin* ____ **1465 – 1468**

Incorporation of Molybdenum Sulfide Cluster Units into a Dawson-Like Polyoxometalate Structure To Give Hybrid Polythiooxometalates

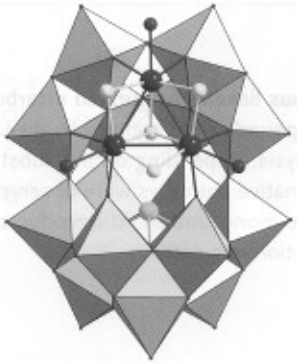

Hybrid polyoxometalates (POMs) $[AsW_{15}Mo_3S_4(H_2O)_3O_{53}]^{9-}$ and $[AsW_{15}Mo_3O_2S_2(H_2O)_3O_{53}]^{9-}$ in which a chalcogenide cluster unit is incorporated into a classical POM structure have been prepared and characterized by X-ray analysis and ^{183}W NMR spectroscopy. The structure of the former can be derived from that of $[H_2AsW_{18}O_{60}]^{7-}$ by replacing one of the six $\{W_3O_{13}\}$ units by a $\{Mo_3S_4O_6(H_2O)_3\}$ unit (see picture; As cyan, Mo blue, O red, S yellow).

Cyclizations

M. L. Grachan, M. T. Tudge, E. N. Jacobsen* ____ **1469 – 1472**

Enantioselective Catalytic Carbonyl–Ene Cyclization Reactions

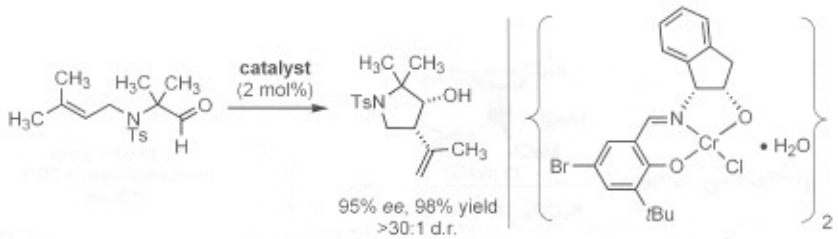

Intramolecular ene reactions of simple alkenyl aldehydes are catalyzed by a chiral (Schiff base)Cr^{III} complex with high enantio- and diastereoselectivity, affording densely functionalized heterocyclic or carbocyclic products (see scheme for example). Desymmetrizations of alkenyl dialdehydes and bis(alkenyl) aldehydes are also achieved.

© 2008 Wiley-VCH Verlag GmbH & Co. KGaA, Weinheim

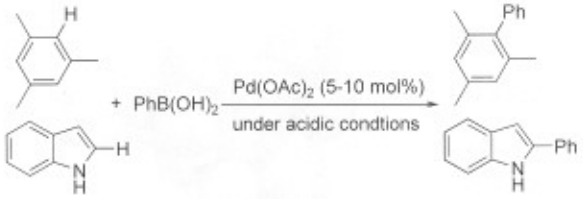

No compass required: A method is described for forming biaryl C–C bonds by a Pd^{II}-catalyzed cross-coupling of aryl C–H bonds with aryl boronic acids under mild conditions without the presence of directing groups. Different substituents on both (hetero)arenes and aryl boronic acids are compatible with the reaction conditions, and the homocoupling of boronic acids is highly inhibited. Dioxygen was applied as the final oxidant.

C–H Activation

S.-D. Yang, C.-L. Sun, Z. Fang, B.-J. Li, Y.-Z. Li, Z.-J. Shi* _____ 1473 – 1476

Palladium-Catalyzed Direct Arylation of (Hetero)Arenes with Aryl Boronic Acids

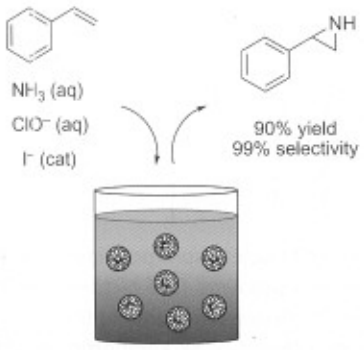

Aziridines from ammonia: Unprotected aziridines are formed from styrenes in one catalytic step. Ammonia is incorporated directly using an aqueous micellar solution containing bleach as oxidant and substoichiometric amounts of iodide (see picture).

Aziridination

C. Varszegi, M. Ernst, F. van Laar, B. F. Sels, E. Schwab, D. E. De Vos* _____ 1477 – 1480

A Micellar Iodide-Catalyzed Synthesis of Unprotected Aziridines from Styrenes and Ammonia

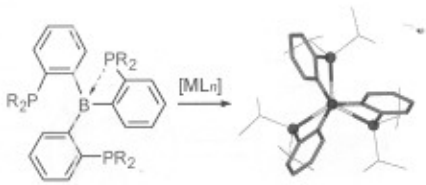

Symmetry from within: Coordination of a triphosphanyl–borane ligand to gold(I) and platinum(0) affords metallaboratranes exhibiting C_3 symmetry both in solution and in the solid state. Such a helical geometry is supported by axial M→B dative interactions and results from the envelope conformations of the PCCBM metallacycles.

Ambiphilic Ligands

S. Bontemps, G. Bouhadir, W. Gu, M. Mercy, C.-H. Chen, B. M. Foxman, L. Maron,* O. V. Ozerov,* D. Bourissou* _____ 1481 – 1484

Metallaboratranes Derived from a Triphosphanyl–Borane: Intrinsic C_3 Symmetry Supported by a Z-Type Ligand

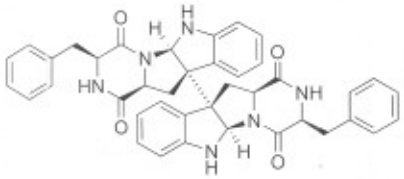

(+)-WIN 64821

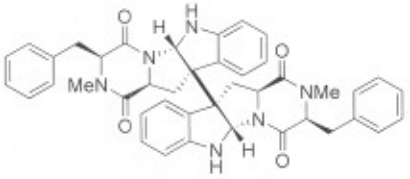

(–)-ditryptophenaline

On a fast track: The secondary metabolites (+)-WIN 64821 and (–)-ditryptophenaline have been synthesized in six and seven steps, respectively, from amino acid derivatives in a concise and enantioselective manner. The gram-scale synthesis of key intermediates and the simultaneous introduction of vicinal quaternary stereocenters are described. The synthesis and structural confirmation of (–)-1′-(2-phenylethylene)ditryptophenaline is also reported.

Natural Product Synthesis

M. Movassaghi,* M. A. Schmidt, J. A. Ashenhurst _____ 1485 – 1487

Concise Total Synthesis of (+)-WIN 64821 and (–)-Ditryptophenaline

© 2008 Wiley-VCH Verlag GmbH & Co. KGaA, Weinheim

Contents

Lanthanum(II) Compounds

P. B. Hitchcock, M. F. Lappert,*
L. Maron,*
A. V. Protchenko* ——— 1488 – 1491

Lanthanum Does Form Stable Molecular Compounds in the +2 Oxidation State

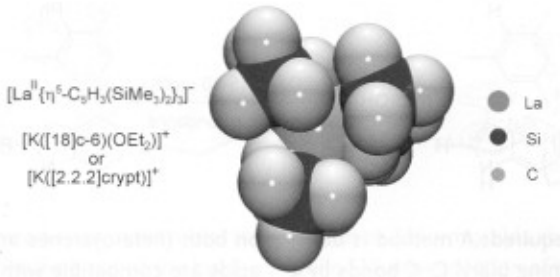

Getting down to business: Reduction of the La^{III} tricyclopentadienide complex $[LaCp''_3]$ ($Cp'' = \eta^5\text{-}1,3\text{-}(SiMe_3)_2C_5H_3$) by K and [18]crown-6 or [2,2,2]cryptand produced thermally stable mononuclear crystalline lanthanate(II) salts. The La +2 oxidation state in these complexes was confirmed both in solution (EPR) and the solid state (EPR, SQUID, X-ray diffraction) and was supported by a computational study.

Heterogeneous Catalysis

K. V. Kovtunov, I. E. Beck, V. I. Bukhtiyarov, I. V. Koptyug* ——— 1492 – 1495

Observation of Parahydrogen-Induced Polarization in Heterogeneous Hydrogenation on Supported Metal Catalysts

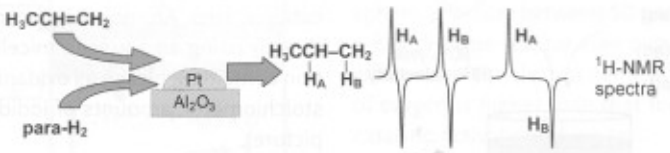

Contrary to popular opinion, two H atoms from the same H_2 molecule can end up in the same product molecule and retain their spin correlation during heterogeneous hydrogenation on supported metal catalysts and thus produce parahydrogen-induced nuclear spin polarization in the reaction products (see picture). For 0.6-nm Pt clusters on alumina, the contribution of the pairwise addition route in the hydrogenation of propylene amounts to at least 3%.

Nanostructures

A. Riss, T. Berger, S. Stankic, J. Bernardi, E. Knözinger, O. Diwald* — 1496 – 1499

Charge Separation in Layered Titanate Nanostructures: Effect of Ion Exchange Induced Morphology Transformation

Clear complementarity: Surface chemistry induced morphology transformation in layered titanate nanostructures can be used to control their photoelectronic properties. $Na_2Ti_3O_7$ nanowires can be transformed reversibly into nanotubes with acid/base treatment (see picture); the nanowires exhibit photoluminescence, which is suppressed in the nanotubes, while the charge separation is stronger in the nanotubes.

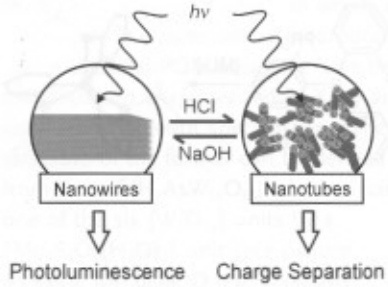

Carbohydrate Synthesis

S. Wendicke, S. Warnecke, C. Meier* ——— 1500 – 1502

Efficient Synthesis of Nucleoside Diphosphate Glycopyranoses

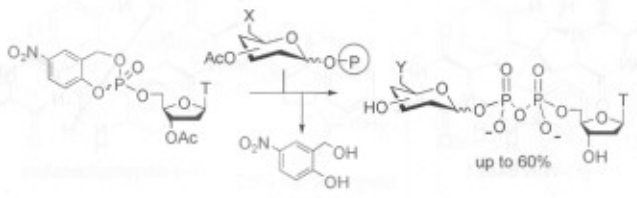

Short and sweet: A new, short synthetic pathway for the synthesis of the enormously important class of nucleoside diphosphate sugars (NDP sugars) was developed using *cyclo*-saligenyl (*cyclo*Sal) nucleosyl phosphate triesters as active ester equivalents that form the target compounds in the presence of anomerically pure pyranose 1-phosphates in high yields (see scheme; T = thymine; X = OAc, H; Y = OH, H).

© 2008 Wiley-VCH Verlag GmbH & Co. KGaA, Weinheim

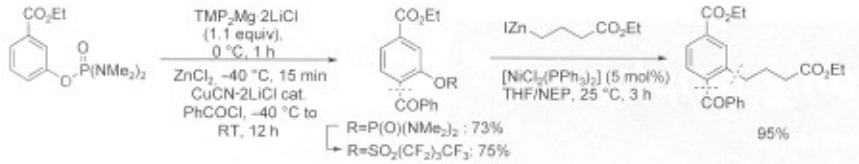

Getting directions: The $(Me_2N)_2P(O)O$ substituent serves as an effective directing-metalation group in the magnesiation of substituted arenes with $TMP_2Mg{\cdot}2\,LiCl$ (see scheme). This reaction can be used to achieve difficult substitution patterens by *meta,para* or *para,meta* functionalization. TMP = 2,2,6,6-tetramethylpiperamidyl, NEP = *N*-ethylpyrrolidone.

Grignard Reactions

C. J. Rohbogner, G. C. Clososki, P. Knochel* ——— 1503 – 1507

A General Method for *meta* and *para* Functionalization of Arenes Using $TMP_2Mg{\cdot}2\,LiCl$

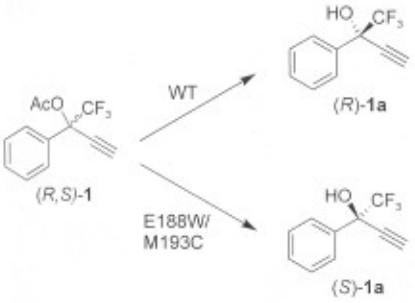

Simultaneous saturation mutagenesis at three amino acid residues of esterase BS2 followed by high-throughput screening identified a double mutant (E188W/M193C) with inverted enantiopreference, high *E* values, and broadened substrate range compared to the wild-type (WT) enzyme, while the single mutants lacked this property. The kinetic resolution of ester **1** with the enzymes is shown in the scheme.

Esterases

S. Bartsch, R. Kourist, U. T. Bornscheuer* ——— 1508 – 1511

Complete Inversion of Enantioselectivity towards Acetylated Tertiary Alcohols by a Double Mutant of a *Bacillus Subtilis* Esterase

Four of the best: Reaction of dimethylzinc with isopropyl carbodiimide at elevated temperature occurs with C–C bond formation and subsequent formation of polynuclear zinc amidinate complexes (see picture for tetranuclear complex, whose ligand is formed by the coupling of four carbodiimide ligands). Such a reaction is without precedent in amidinate chemistry.

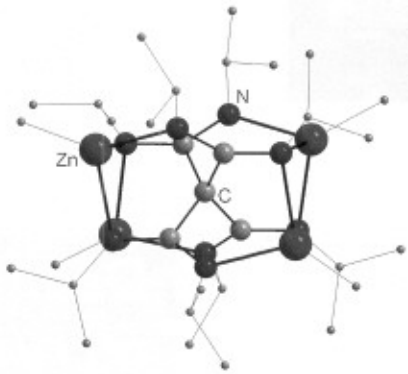

Zinc Amidinate Complexes

M. Münch, U. Flörke, M. Bolte, S. Schulz,* D. Gudat ——— 1512 – 1514

Unexpected C–C Bond Formation and Synthesis of Tetranuclear Zinc Carbodiimide Clusters from the Reaction of $ZnMe_2$ and *i*PrN=C=N*i*Pr

Dumbbells that block: Dnmt1 is a crucial enzyme in maintaining the methylation pattern of genes and as such is a critical element of the epigenetic programming process. DNA dumbbell constructs have been developed that inhibit Dnmt1 and have potential in the regulation of DNA methylation patterns in cells (see scheme; SAM = S-adenosylmethionine, Fl = Cy3 fluorescence label, C^N = 5-azadC, C-Me = 5-methyldC).

DNA Methylation

D. Kuch, L. Schermelleh, S. Manetto, H. Leonhardt, T. Carell* ——— 1515 – 1518

Synthesis of DNA Dumbbell Based Inhibitors for the Human DNA Methyltransferase Dnmt1

Supporting information is available on the WWW (see article for access details).

A video clip is available as Supporting Information on the WWW (see article for access details).

© 2008 Wiley-VCH Verlag GmbH & Co. KGaA, Weinheim